Physica B 684 (2024) 415969

Contents lists available at ScienceDirect

Physica B: Condensed Matter

journal homepage: www.elsevier.com/locate/physb

Structural characterization of silver nanoparticles produced by biogenic synthesis using SAXS

Ari Ribeiro Junior [a], Fabiano Yokaichiya [a], Eneli Monerjan [b], Karina Lemke [b], Mariana Guilger-Casagrande [c,d], Renata Lima [c], Leonardo Fraceto [d], Margareth K.K.D. Franco [e,*], Guinther Kellermann [a]

[a] Universidade Federal do Paraná, Department of Physics, Curitiba, Brazil
[b] Helmholtz-Zentrum Berlin für Materialien und Energie (HZB), Germany
[c] Universidade de Sorocaba, Sorocaba, Brazil
[d] Universidade Estadual Paulista Júlio de Mesquita Filho, Bauru, Brazil
[e] Instituto de Pesquisas Energéticas e Nucleares, São Paulo, Brazil

ARTICLE INFO

Keywords:
SAXS
Biogenic silver nanoparticles
Trichoderma harzianum
Sclerotinia sclerotiorum

ABSTRACT

Nanotechnology applied to the agricultural sector has highlighted in recent decades, making important contributions, including systems for pest control as biogenic nanoparticles. These nanoparticles are used to control phytopathogens, demonstrating the need to understand its composition, mechanisms of action and toxicity. Their capping of biomolecules, derived from the organism used in the synthesis, contributes to their stability and biological activity. Ag nanoparticles were produced by the fungus *Trichoderma harzianum* in aqueous solutions containing silver nitrate as a precursor for the silver nanoparticles. Some of the samples were exposed to the phytopathogenic fungus *Sclerotinia sclerotiorum* responsible for the white mold. After preparation, a fraction of the samples was submitted to physico-chemical processes to remove organic cap layer on nanoparticles surface formed during the preparation process. In this study we determined the effect of the phytopathogenic fungus and cap removal process in the average radius, radius dispersion, number density of the nanoparticles using small angle X-ray scattering (SAXS), where we considered their almost spherical shape in aqueous solution obtained by the biogenic route. The SAXS data analyses suggest that the presence of the pathogenic fungus results in a diminution of number and total volume of Ag NPs without significant effects on average radius and radius dispersion. Our results also indicate that the physic-chemical process to remove the organic cap surrounding the Ag NPs leads to a decrease in the fraction of the smaller nanoparticles.

1. Introduction

Nanotechnology is an innovative scientific term used in areas such as food production, agriculture, cosmetic, medicine, textile and pharmaceutical industry [1]. It will facilitate the development phases of genetically modified crops, inputs for livestock and fishing activities, more precise agricultural methods and the development of environmentally friendly pesticides. Among the research areas of nanotechnology there are those involving metallic nanoparticles. Some metals present changes in their physicochemical properties at the nanometer scale, partially due to an increase in their surface area. Metallic nanoparticles, such as silver nanoparticles (Ag NPs), have numerous applications mainly due to their antibacterial activity [2]. Silver nanoparticles are also characterized by being in a size range between 1 nm and 100 nm [3].

One of the most common means of producing metallic nanoparticles is through chemical and physical processes, but these methods use toxic solvents, hazardous by-products and high energy consumption. On the other hand, green biological synthesis methods [4,5] have been showing promising results in the field of research, these methods have great potential in the production of metallic nanoparticles where it is possible to obtain them at a low cost, in an energetically efficient and non-toxic process. One of the main advantages that can be highlighted is the possibility of increasing the scale of production. In this study, the green biological synthesis method using fungi to produce Ag nanoparticles is extremely efficient, providing economic viability and biomass

* Corresponding author. Av. Lineu Prestes 2342, Cidade Universitária Armando Sales de Oliveira, São Paulo, SP, CEP 05508-900, Brazil.
E-mail address: margareth_franco@yahoo.com.br (M.K.K.D. Franco).

https://doi.org/10.1016/j.physb.2024.415969
Received 4 December 2023; Received in revised form 3 April 2024; Accepted 13 April 2024
Available online 14 April 2024

management [6].

In the biosynthesis of metallic nanoparticles by a fungus, its mycelium is exposed to a metallic salt solution, leading the fungus to produce enzymes and metabolites for its own survival. In this process, metal ions are reduced to solid metallic nanoparticles through the catalytic effect of the extracellular enzyme and metabolites of the fungus [7].

One of the biggest problems with Ag NPs is their stability. The smaller the nanoparticle, the greater it's total surface area, favoring the aggregation into larger particles through metal-metal bonds, which is not desirable [8]. An advantage in biogenic synthesis is the creation of a natural coating (cap) on the nanoparticles, composed of biomolecules and other compounds derived from the metabolism of the fungus or other biological agent, such as enzymes, amino acids, extracellular proteins and secondary metabolites. This process, in addition to increasing the stability of the compound, also makes the nanoparticle more compatible with biological tissues, providing applications in the areas of health, agriculture and the environment [9].

The study of the Ag NPs, prepared using the *Trichoderma harzianum* fungus, a microparasitic filamentous fungus, is of great importance as a biological control agent against phytopathogens that affect the production of several plant species of agricultural importance, as observed in recent researches [10–12]. The *Trichoderma harzianum* fungus main mechanism of action is through the growth of hyphae and the release of hydrolytic enzymes that degrade the cell wall of the target fungus. Results obtained from the Ag NPs produced by this synthesis showed that the capped samples are more effective against the fungus *Sclerotinia sclerotiorum* compared to the non-capped ones [9].

The aim of this study is to characterize the Ag NPs in aqueous solution obtained by different treatments via the biogenic route of the fungus *Trichoderma harzianum* using SAXS technique, and its data analysis will allow a better understanding of some of the structural parameters obtained from Ag NPs.

2. Experimental

Ag NPs were obtained in a water solution by a biogenic synthesis method using a EcotrichTM product, the Trichoderma harzianum (TH) fungus culture. The concentration used in the field (0.127 mg/mL) was plated on PDA medium, followed by cultivation at room temperature, in the dark, for 6 days. The mycelium discs were transferred to Potato-Dextrose Broth (PD) and cultivated for 12 days, with shaking at 150 rpm57, after growth. Next, the biomass was filtered, transferred to ultrapure water and kept under stirring for 72 h, then finally vacuum filtered and discarded. Silver nitrate ($AgNO_3$) was added to the filtrate solution containing the fungus at a concentration of 1×10^{-3} mol/L and kept under stirring until the color changed from light yellow to dark brown, confirming the synthesis.

In order to investigate the effect of the *Sclerotinia sclerotiorum* fungus in size and number of Ag NPs, this fungus was added to a fraction of the solution containing the *Trichoderma harzianum* (TH) fungus. As demonstrated in previous studies, the Ag NPs obtained using these preparation methods have nearly spherical shape and present an organic cap evolving each nanoparticle [13]. After the nanoparticle production, part of these solutions (with and without the *Sclerotinia sclerotiorum* fungus) were submitted to physical-chemical processes to remove the organic cap covering, the Ag NPs without cappings were obtained by boiling the pellets in 60 mM Tris-HCl pH 6.8, followed by dialysis using a Visking MWCO 12–14 kDa membrane [9]. Fig. 1 shows a scheme of the processes used to prepare the four samples here investigated.

SAXS measurements were performed on a SAXSess instrument (Anton Paar) equipped with a one-dimensional position-sensitive detector (Mythen 2R, Dectris). A Ni filter was used to suppress the Cu K_β-contribution. The SAXS intensity curves were obtained as a function of the modulus of the scattering vector $q = 4\pi\sin\theta/\lambda$, where θ is half of the scattering angle and $\lambda = 0.1540$ nm the X-rays wavelength (Cu-K_α). This instrument utilizes a primary X-ray beam whit line shaped cross-section in order to provide higher intensity. The desmearing of the intensity curves to account for the beam cross-section was performed using the algorithm developed by Strobl (1970) [14] with improved numerical stability [15] including error propagation. The liquid solutions containing the nanoparticles were injected in a borosilicate capillary whit 0.78 mm in diameter with its axis aligned along the largest dimension of the X-ray beam cross-section. Prior to measurement, the sample-to-detector path chamber was evacuated (0.5 mbar) to suppress absorption and scattering of the X-rays by the air. The SAXS intensity curves $I \times q$ was measured within the 0.1–1.7 nm^{-1} q-range where the analyzed curve comprises up to q=1.3 nm^{-1}. The data were corrected for sample transmission and detector sensitivity. The contribution to

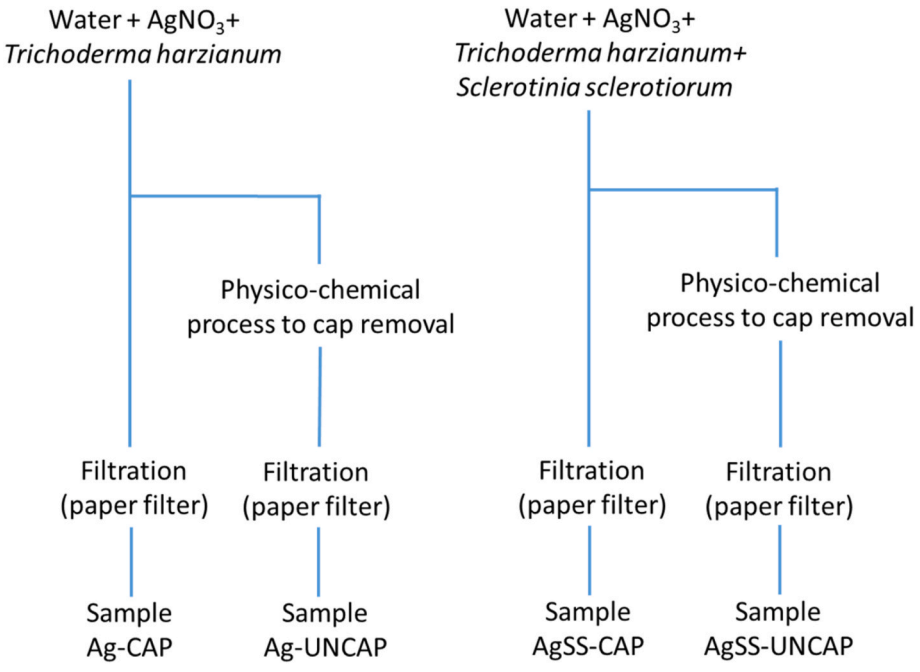

Fig. 1. Scheme of the processes used in the preparation of Ag NPs using biogenic synthesis.

SAXS intensity due to the solution and parasitic scattering was measured and subtracted from the total intensity.

3. Results and discussion

For a diluted set of spherical nanoparticles with electron density ρ embedded in a homogenous solution with electron density ρ_0, the SAXS intensity is given by Ref. [16]:

$$I(q) = (\rho - \rho_0)^2 \int_0^\infty |F(qR)|^2 [v(R)]^2 N(R) dR, \quad (1)$$

where $v(R) = 4\pi R^3/3$ is the volume of the particle with radius R. $N(R)$ is the radius distribution function, $N(R)dR$ being the number of nanoparticles with a radius between R and $R + dR$ and $F(qR)$ is the scattering amplitude of a spherical nanoparticle, given by:

$$F(q,R) = 3\frac{sin(qR) - qRcos(qR)}{(qR)^3} \quad . \quad (2)$$

Equations (1) and (2) gives the SAXS intensity the uncapped Ag NPs embedded in the water solution. On the other hand, in general these equations do not apply to a three phase system consisting in nanoparticles having core-shell structure embedded a solution. However, in the system investigated in which the electron density of the Ag NPs is much higher than that of the organic cap, the effect of the cap surrounding the nanoparticles is expected to be very small. Therefore, in our analysis we assumed that Equations (1) and (2) are valid approximations to describe the SAXS intensity of all studied samples. As will be shown, this assumption is corroborated by the good agreement between the experimental and calculated SAXS intensity using these equations.

Fig. 2 shows the SAXS intensity curves as a function of the modulus of the scattering vector q for the four studied samples. Differences in shape of these curves can be assigned to differences in the size of the Ag NPs.

In order to determine the radius distribution function of the Ag NPs we used the GNOM [17] program from ATSAS package [18]. As an output, GNOM provides the volume distribution function $V(R)$ of the Ag nanoparticles, that is related to radius distribution function by $N(R) = V(R)/v(R)$. Fig. 3 shows the radius distribution functions $N(R)$ determined by the GNOM program applied to the SAXS intensity curves shown in Fig. 2. The continuous lines in Fig. 2 are the SAXS intensity corresponding to the $N(R)$ functions in Fig. 3.

Fig. 4 shows the average radius $\langle R \rangle$, radius dispersion σ, number n and total volume V_{tot} of the Ag nanoparticles in relative units for the four samples calculated from the radius distribution function.

We can see in Fig. 4 that the number n and total volume V_t (in relative units) of the Ag NPs in the samples containing the capped nanoparticles are much higher than those in the samples where the cap layer was removed. On the other hand, the average radius of these nanoparticles is smaller than that of uncapped samples. These results suggest that the physical-chemical processes used to remove the cap layer may have also removed a large part of the smaller particles.

It was observed that the procedure of having enzyme production stimulated by the presence of the cell wall of the *Sclerotinia sclerotiorum* fungus resulted in a significant decrease in the volume fraction and number of capped silver nanoparticles. This process, however, did not significantly affect the values of the average radius and radius dispersion.

We also noticed that the dispersion in size of the uncapped nanoparticles is much smaller than that of the capped ones. This behavior, together with the increase in the average radius of the Ag NPs in samples submitted to the cap removal process, provides additional evidence to conclude that the process used to remove the cap from the surface of Ag nanoparticles leaded to an exclusion of a significant fraction of the smaller Ag NPs. The SAXS results presented in this study corroborate Scanning Electron Microscopy (SEM) and Dynamic Light Scattering (DLS) measurements performed and presented previously elsewhere [9].

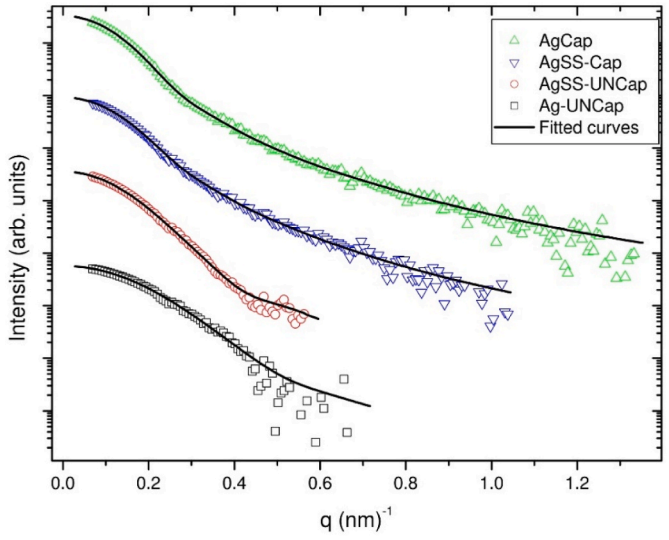

Fig. 2. SAXS intensity curves from Ag NPs obtained from the filtration of a solution prepared by biogenic synthesis using the fungus *Trichoderma harzianum*. The labels AgSS-CAP and AgSS-UNcap corresponds to samples in which enzyme production was stimulated by the phytopathogenic *Sclerotinia sclerotiorum* fungus with and without an external cap formed on nanoparticles surface, respectively. Ag-UNCAP and Ag-CAP are the samples for whit and without enzyme stimulation for which the external cap formed around the NPs was removed using physic-chemical processes.

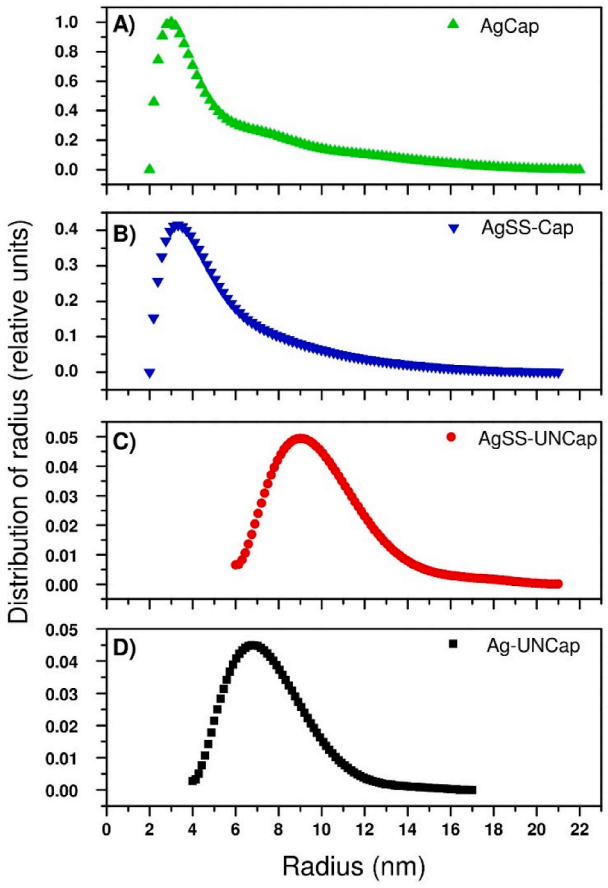

Fig. 3. Radius distribution function $N(R)$ of the Ag nanoparticles determined from the SAXS intensity curves shown in Fig. 2.

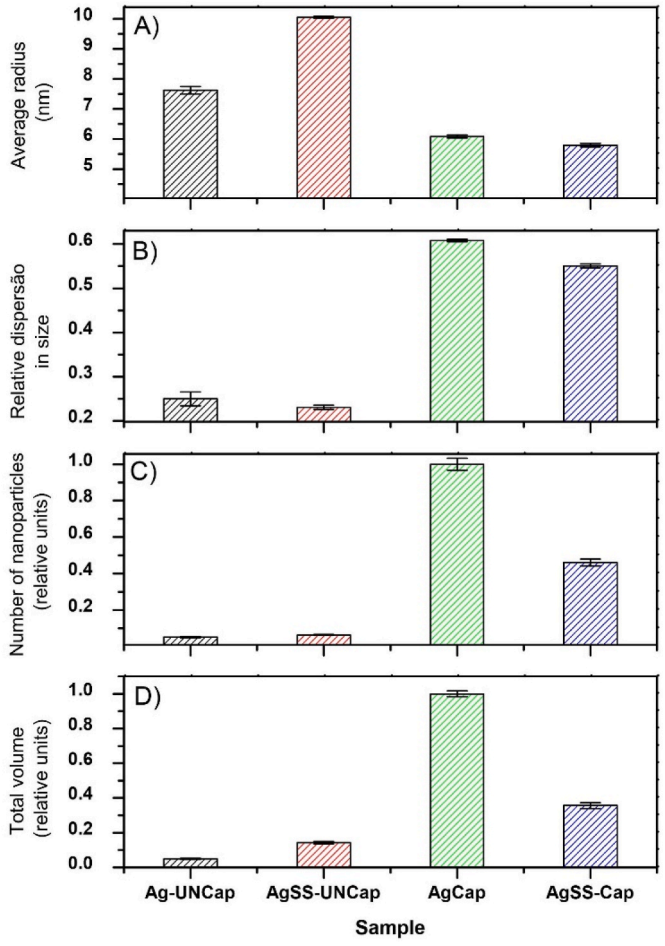

Fig. 4. (A) Average radius, (B) radius dispersion, (C) number and (D) total volume in relative units of the Ag nanoparticles determined from the SAXS intensity for the four investigated samples.

4. Conclusion

In this study, we performed a low-resolution structural characterization of Ag NPs produced in a water solution by biogenic synthesis methods using the SAXS technique. The nanoparticles were produced from the fungus *Trichoderma harzianum* and $AgNO_3$. A part of the samples was synthesized by exposing this fungus to the pathogenic fungus *Sclerotinia sclerotiorum*, which causes white mold. A fraction of the samples prepared with and without the pathogenic fungus were also submitted to physical-chemical processes to remove the organic layer that surrounds the nanoparticles. From the analysis of the scattering curves, we determined the radius distribution of the Ag NPs prepared using the four different processes.

The analysis of the SAXS curves allowed us to determine the average radius, dispersion in radius, number and total volume (in relative units) occupied by the nanoparticles. The results suggest that the presence of the pathogenic fungus results in a diminution of number and total volume of Ag NPs without significant effects on average radius and radius dispersion. Our results also indicated that the physic-chemical process used to remove the organic cap surrounding the Ag NPs leads to a decrease in the fraction of the smaller nanoparticles.

CRediT authorship contribution statement

Ari Ribeiro Junior: Formal analysis. **Fabiano Yokaichiya:** Writing – original draft, Formal analysis. **Eneli Monerjan:** Investigation. **Karina Lemke:** Investigation. **Mariana Guilger-Casagrande:** Conceptualization. **Renata Lima:** Resources, Conceptualization. **Leonardo Fraceto:** Resources, Conceptualization. **Margareth K.K.D. Franco:** Writing – original draft, Formal analysis. **Guinther Kellermann:** Formal analysis.

Declaration of competing interest

All persons who meet authorship criteria are listed as authors, and all authors certify that they have participated sufficiently in the work to take public responsibility for the content, including participation in the concept, design, analysis, writing, or revision of the manuscript. Furthermore, each author certifies that this material or similar material has not been and will not be submitted to or published in any other publication before its appearance in the Physica B.

Data availability

Data will be made available on request.

Acknowledgment

L.F.F, R.L and M.G.-C. would like to thank the financial support provided by the INCT Nanotechnology for Sustainable Agriculture, National Council for Scientific and Technological Development (MCTI-CNPq- INCTNanoAgro #405924/2022-4); Coordination for the Improvement of Higher Education Personnel – Brazil (MEC-CAPES INCTNanoAgro #88887.953443/2024-00); São Paulo Research Foundation (FAPESP grant, 2017/21004- 5; # 22/03399-0; # 20/05816-2, CEPID CBioClima #2021/10639-5).

References

[1] S. Mobasser, A.A. Firoozi, Review of nanotechnology applications in science and engineering, Journal Civil Eng. Urban (2016) 84–93.
[2] A. El-Nour, M.M. Kholoud, et al., Arabian journal of chemistry, "Synthesis and applications of silver nanoparticle" 3 (3) (2010) 135–140.
[3] C. Graf, D.L.J. Vossen, A. Imhof, A. Van Blaaderen, Langmuir, "A general method to coat colloidal particles with silica" 19 (17) (2003) 6693–6700, https://doi.org/10.1021/la0347859.
[4] G. Vassyliev, V. Vorobyova, Valorization of food waste to produce eco-friendly means of corrosion protection and green synthesis of nanoparticles, Adv. Mater. Sci. Eng. (2020) 6615118, https://doi.org/10.1155/2020/6615118.
[5] V. Khimii, K. Tekhnologii, Вопросы хиМии и хиМической технологии, Preparation of silver nanoparticles by contact nonequilibrium low-temperature plasma in the presence of sodium alginate 6 (2017) 82–88.
[6] K.N. Thakkar, S.S. Mhatre, R.Y. Parikh, Nanomedicine: nanotechnology, biology and medicine, Biological synthesis of metallic nanoparticles 6 (2) (2010) 257–262.
[7] R.M. Elamawi, R.E. Al-Harbi, A.A. Hendi, Egyptian Journal of Biological Pest Control, "Biosynthesis and characterization of silver nanoparticles using Trichoderma longibrachiatum and their effect on phytopathogenic fungi", 28, 1, 28-32. ISSN 2536-9342, doi: 10.1186/s41938-018-0028-1.
[8] K.J. Klabunde, Nanoscale materials in chemistry, J. Am. Chem. Soc. 124 (35) (2001) 10629–10630, https://doi.org/10.1021/ja0252072.
[9] M. Guilger Casagrande, T. Germano Costa, N. Bilesky-Jose, T. Pasquoto-Stigliani, L. Carvalho, L.F. Fraceto, R. de Lima, Influence of the capping of biogenic silver nanoparticles on their toxicity and mechanism of action towards Sclerotinia sclerotiorum, J. Nanobiotechnol. 19 (1) (2021) 53–56, https://doi.org/10.1186/s12951-021-00797-5. ISSN 1477-3155.
[10] A. Jomeyazdian, M. Primia, H. Alaei, A. Taheri, S. Sarani, Control of Fusarium wilt disease of tomato and improvement of some growth factors through green synthesized zinc oxide nanoparticles, Research Square (2024), https://doi.org/10.1007/s10658-024-02831-2.
[11] P. Sanguinedo, R. Faccio, E. Abreo, S. Alborés, Biogenic Silver and Copper Nanoparticles: potential antifungal agnts in rice and wheat crops, Chemistry 5 (2023) 2104–2119, https://doi.org/10.3390/chemistry5040143.
[12] A. Athaafah Tomah, Z. Zhang, I.S. Alamer, A. Khattak, T. Ahmed, Minjun Hu, D. Wang, L. Xu, B. Li, Y. Wang, "The potential of trichoderma-mediated nanotechnology application in sustainable development scopes", Nanomaterials 13 (2023) 2475, https://doi.org/10.3390/nano13172475.
[13] M. Guilger, T. Pasquoto-Stigliani, N. Bilesky-Jose, R. Grillo, P.C. Abhilash, L. F. Fraceto, R.D. Lima, Biogenic silver nanoparticles based on trichoderma harzianum: synthesis, characterization, toxicity evaluation and biological activity, Sci. Rep. 7 (1) (2017) 44421–44426. ISSN 2045-2322.
[14] G.R. Strobl, A new method of evaluating slit-smeared small-angle X-ray scattering data, Acta Crystallogr., Sect. A 26 (1970) 367–375, https://doi.org/10.1107/S0567739470000888.

[15] M. Soliman, B.-J. Jungnickel, E. Meister, Acta Crystallogr. Sect. A Found. Crystallogr, "Stable Desmearing of Slit-Collimated SAXS Patterns by Adequate Numerical Conditioning 54 (1998) 675–681, https://doi.org/10.1107/S010876739800573X.
[16] A. Guinier, G. Fournet, C. Walker, Small-angle Scattering of X-Rays. [S.l.], Wiley, 1955 (Structure of matter series).
[17] D.I. Svergun, J. Appl Crystallogr, Determination of the Regularization Parameter in Indirect-Transform Methods Using Perceptual Criteria, vol. 25, 1992, pp. 495–503.
[18] K. Manalastas-Cantos, P.V. Konarev, N.R. Hajizadeh, A.G. Kikhney, M. V. Petoukhov, D.S. Molodenskiy, A. Panjkovich, H.D.T. Mertens, A. Gruzinov, C. Borges, C.M. Jeffries, D.I. Svergun, D. Franke, D.J. Appl, Atsas 3.0: expanded functionality and new tools for small-angle scattering data analysis, Cryst. 54 (2021) 343–355.